

A New Analytical Model of the Brake Pad for Improved Calculation of the Centre of Pressure and Friction Coefficient in A Multi-Piston Disc Brake

Tomas Budinsky*, Peter Brooks and David Barton

School of Mechanical Engineering
University of Leeds, Leeds, United Kingdom
*Corresponding author Email: mntb@leeds.ac.uk

Abstract

In recent experimental work it has been observed that the position of the centre of pressure (CoP) at the brake pad/disc interface has an influence on the onset of brake squeal. To determine the CoP during a braking event, a simple two-dimensional analytical model of the brake pad or more complex numerical finite element model of a disc brake are commonly used. This paper presents a new three-dimensional analytical model of a brake pad that determines the CoP position in both circumferential and radial directions. Due to higher complexity, this model provides more realistic clamp and friction force values, which can be used together with the more accurate radial position of the CoP for evaluation of the brake torque. The CoP position calculated using the new model was compared with the CoP evaluated by a finite-element model of an equivalent 8-piston opposed disc brake. The CoP results across the whole pad/disc interface showed a close correlation between these two approaches, giving the new analytical model a potential use in applications where an instantaneous value of the CoP with good accuracy is required. Finally, the new model was used to demonstrate possible improvement of the traditional method of the friction coefficient calculation. Due to greater accuracy the new model gives an approximately 8% larger value of the friction coefficient than the traditional approach.

Keywords: Analytical model; Brake pad; Centre of pressure; Effective radius; Friction coefficient; Multi-piston disc brake

1. Introduction

Even though brake squeal has been intensively studied and numerous techniques have been proposed to eliminate this undesirable phenomenon during the last century, it still represents a major concern for the automotive brakes industry. This is mostly due to the interdisciplinary complexity of the problem where numerous physical phenomena occur at the same time and are difficult to predict even with use of current computational technology. The research focus is especially targeted to the squeal frequency range of 1-16 kHz, which is considered to be the most disturbing for the vehicle occupants [1]. Now, it is well accepted within the brake research community that the brake squeal results from the friction-induced vibration of the brake assembly [2].

In recent experimental work, it has been observed that the position of the centre of pressure (CoP) at the brake pad/disc contact area has an influence on the onset of brake squeal [3]. Also, subsequent experimental studies [4], [5] showed a certain correlation between the squeal occurrence and the position of the CoP. Therefore, an increased interest exists in studying the contact pressure distribution along with the CoP position at the pad/disc interface and their impact on vibrational behavior of the brake system.

The CoP position can be investigated either experimentally using pressure or force sensors integrated in the brake pad, numerically by developing a three-dimensional (3D) finite element model or

analytically using an appropriate analytical model. Even though numerous analytical models of disc brakes have been developed to investigate their frequency response, analytical studies of the brake pad/disc interface are rather scarce. Probably the first analytical study was undertaken by Newcomb and Spurr [6] who examined the brake pad/disc pressure distribution and the effect of wear on the effective radius. Fieldhouse et al. [7] also used analytical modeling techniques, deriving two-dimensional (2D) models of brake pads featuring different types of abutments.

The CoP position can be also viewed as the instantaneous position of the reaction (clamp) force and the friction force at the pad/disc interface. This assumption can be used to determine the effective radius of the brake torque. Since this radius has direct impact on the accuracy of the friction coefficient calculation, some researchers have tried to establish methods to improve the determination of the brake effective radius. Besides the indirect CoP measurements using force or pressure sensors, a thermograph analysis is another common approach to investigate the effective radius. Neis et al. [8] and Lange et al. [9] used this method to determine the effective radius by evaluating the radial thermal profile.

In this paper, a new 3D analytical rigid body model of a brake pad is proposed that enables determination of the CoP position at the pad/disc interface in both longitudinal and radial direction, and yields also values of reaction forces acting on the pad. This model is mathematically described in the form of algebraic equations that can be easily solved by means of modern numerical techniques,

and therefore it can be used in simulations where instant values of the CoP position in both longitudinal and radial direction are needed. In the following section, all equations for a 2D and 3D analytical model of the brake pad are derived, followed by an example calculation using realistic data. Then, a similar set of equations are presented for a brake pad with eight opposed pistons to show that the new model can include an arbitrary number of pistons. The longitudinal position of the CoP is first compared with a simple 2D analytical model of the brake pad that has been already described in literature. In order to validate the CoP position in the radial direction, a reduced finite element model of a disc brake with eight opposed pistons is also developed, allowing individual piston control and hence placing the CoP almost arbitrarily over the whole pad/disc area. By maintaining equal testing conditions for both models, the CoP positions can then be directly compared.

Friction coefficient is a common parameter to be defined during the brake system development. The traditional method of friction coefficient calculation includes use of a measured brake torque value, piston pressure and calculated effective radius, where the effective radius is usually assumed to be the mean rubbing surface radius. In this paper, it is proposed to determine the friction coefficient using the new 3D analytical model that yields due to greater complexity more accurate values of the effective radius and clamp force. The new proposed and traditional approaches are compared in the final section of this study, followed by the conclusions.

2. Calculation of Centre of Pressure (COP) Using Analytical Modelling Approaches

A simple rigid body model of a brake pad is usually used to investigate the position of CoP without any need for excessive modeling effort. Analytical models mostly neglect flexural behaviour of the brake pad, temperature effects, wear, and replace complicated surface interactions with individual forces acting at a single point. Therefore, the calculation time of such models is relatively short, which gives the possibility to use them in real-time applications. On the other hand, recent numerical finite-element models have shown what additional effects arise at the brake pad/disc interface, giving a potential for further development of analytical models.

The following analytical models include only one brake pad, allowing to model the inboard and outboard side of a disc brake individually. For a sake of simplicity it will be assumed that both sides are identical.

2.1. 2D Analytical Model of the Brake Pad

A two-dimensional (2D) analytical model of the brake pad for calculation of CoP has been already developed in the literature [7]. Here, a similar model for a four-piston opposed caliper with a trailing abutment is derived. A 2D analytical modelling approach assumes that all forces are co-planar and the friction forces at the backplate/piston interface are neglected. Figure 1 shows the relevant free body diagram of the brake pad with a trailing abutment for a four-piston opposed caliper. The sum of the forces for static equilibrium can be written as follows:

$$x: P_1 + P_2 - F_{tA} - R = 0 \quad (1)$$

$$y: R_A - F_t = 0 \quad (2)$$

and for moment equilibrium with respect to the z axis:

$$M_z: R_{yR} - F_t \left(t_{fm} + \frac{t_{bp}}{2} \right) + P_1 n_1 - P_2 n_2 - F_{tA} y_A = 0 \quad (3)$$

Substituting Eqn. (1) into Eqn. (3) and since

$$F_t = R\mu \quad F_{tA} = R_A\mu_A \quad R_A = F_t \quad (4)$$

the position of CoP can be derived as:

$$y_R = \mu\mu_A y_A + \mu \left(t_{fm} + \frac{t_{bp}}{2} \right) + \frac{(-P_1 n_1 + P_2 n_2)(1 + \mu\mu_A)}{P_1 + P_2} \quad (5)$$

where μ is the friction coefficient at the pad/disc interface, μ_A denotes the friction coefficient at the backplate/abutment surface, y_A represents distance of the pad center to the abutment surface, P_1 and P_2 are piston forces, F_t and R are friction force and reaction force (clamp force) at the rubbing surface, respectively, F_{tA} and R_A are friction force and reaction force at the abutment surface, respectively, n_1 and n_2 represent distances of the pistons from the center of the pad, and t_{fm} and t_{bp} are thicknesses of the friction material and the backplate, respectively.

2.2. New 3D Analytical Model of the Brake Pad for a 4-Piston Opposed Caliper

In the previous 2D analysis, only the circumferential position of the CoP can be calculated, whereas the 3D analysis also allows determination of the CoP position in the radial direction.

First, equations for the new 3D model are derived for an example of a four-piston opposed disc brake, where the contact between the backplate and the trailing abutment is in compression. A relevant 3D free body diagram of the brake pad is shown in Figure 2, assuming an XYZ coordinate system placed at a distance r_{pad} from the disc axis and located in the middle of the backplate. In the Y-Z plane, the pad is modelled as a binary member, i.e. the trailing abutment reaction is represented by a single force acting at the trailing edge interface which is always collinear with the friction force acting at the CoP. Any contact of the backplate with the abutment at the leading edge is neglected. These assumptions enable a solution to the set of equations derived below. Similarly to the 2D analysis, the friction forces at the piston/backplate interface are neglected and the contact between the backplate and the trailing abutment is modelled as a sliding friction contact.

Again, μ and μ_A represent friction coefficients at the pad/disc and pad/abutment interface, respectively, y_A is the horizontal distance from the pad center to the abutment point, z_A is the vertical distance from the pad center to the abutment point, P_1 and P_2 are piston forces, F_{tY} , F_{tZ} and R are friction forces and reaction force (clamp force) at the rubbing surface, respectively, F_{tA} , R_{AY} and R_{AZ} are friction force and reaction forces at the abutment surface, respectively, n_1 and n_2 are distances of the pistons from the center of the pad, t_{fm} and t_{bp} are thicknesses of the friction material and the backplate, respectively. Furthermore, r_{pad} is the vertical distance of the pad axis system to the rotor axis, r is the instantaneous distance of the CoP to the rotor center (effective radius) and α is the angle between the line intersecting the CoP with the rotor axis and the z-axis of the coordinate system. The sum of the forces for static equilibrium can be written as follows:

$$x: P_1 + P_2 - F_{tA} - R = 0 \quad (6)$$

$$y: R_{AY} - F_{tY} = 0 \quad (7)$$

$$z: F_{tZ} - R_{AZ} = 0 \quad (8)$$

The equations of moment equilibrium with respect to the axis system XYZ are:

$$M_x: -R_{AZ} y_A + R_{AY} z_A + F_{tY} (r_{pad} - r \cos \alpha) - F_{tZ} r \sin \alpha = 0 \quad (9)$$

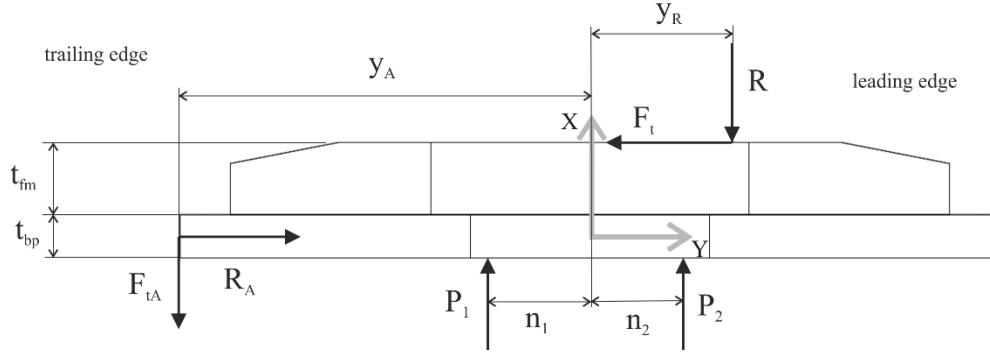


Fig. 1: Simple 2D model of the brake pad for calculation of the CoP position at the pad/disc interface.

$$M_y: F_{tA}z_A - R(r_{\text{pad}} - r \cos \alpha) + F_{tZ} \left(t_{\text{fm}} + \frac{t_{\text{bp}}}{2} \right) = 0 \quad (10)$$

$$M_z: Rr \sin \alpha - F_{tY} \left(t_{\text{fm}} + \frac{t_{\text{bp}}}{2} \right) + P_1 n_1 - P_2 n_2 - F_{tA} y_A = 0 \quad (11)$$

Substituting the following expressions into Eqn. (6) – Eqn. (11)

$$F_t = R\mu \quad F_{tA} = R_{AY}\mu_A \quad F_{tY} = F_t \cos \alpha \quad F_{tZ} = F_t \sin \alpha \quad (12)$$

And since

$$z_A = (y_A + r \sin \alpha) \tan \alpha + r \cos \alpha - r_{\text{pad}} \quad (13)$$

$$R_{AY} = F_{tY} \quad F_{tZ} = R_{AZ} \quad (14)$$

The system of equations can be written as follows:

$$R = \frac{P_1 + P_2}{1 + \mu_A \mu \cos \alpha} \quad (15)$$

$$r = \frac{-\mu \mu_A \cos \alpha (-r_{\text{pad}} + y_A \tan \alpha) + r_{\text{pad}} - \mu \sin \alpha \left(t_{\text{fm}} + \frac{t_{\text{bp}}}{2} \right)}{\mu \mu_A + \cos \alpha} \quad (16)$$

Substituting Eqn. (12) and Eqn. (14) into Eqn. (11) yields

$$R \left(r \sin \alpha - \mu \cos \alpha \left(t_{\text{fm}} + \frac{t_{\text{bp}}}{2} \right) - y_A \mu \mu_A \cos \alpha \right) + P_1 n_1 - P_2 n_2 = 0 \quad (17)$$

Finally, substituting Eqn. (15) and Eqn. (16) into Eqn. (17) and rearranging gives Eqn. (18)

$$\begin{aligned} & \frac{P_1 + P_2}{1 + \mu_A \mu \cos \alpha} \left(\frac{-\mu \mu_A \cos \alpha (-r_{\text{pad}} + y_A \tan \alpha)}{\mu \mu_A + \cos \alpha} \sin \alpha + \dots \right. \\ & \left. + \frac{r_{\text{pad}} - \mu \sin \alpha \left(t_{\text{fm}} + \frac{t_{\text{bp}}}{2} \right)}{\mu \mu_A + \cos \alpha} \sin \alpha + \dots \right) \\ & - \mu \cos \alpha \left(t_{\text{fm}} + \frac{t_{\text{bp}}}{2} \right) - y_A \mu \mu_A \cos \alpha + P_1 n_1 - P_2 n_2 = 0 \quad (18) \end{aligned}$$

Eqn. (18) is a non-linear trigonometric equation that includes the unknown angle α . This can be solved numerically in MATLAB[®] using some of the built-in mathematical functions based on a combination of bisection, secant, and inverse quadratic interpolation methods. Due to the nature of trigonometric equations having a repeated periodical solutions, a possible

solution of Eqn. (18) needs to be limited to a small interval to get a meaningful solution for the angle α , e.g. $-0.4 < \alpha < 0.4$ rad. Once the angle α is determined, the radius r on which the resultant friction force is acting can be calculated by substituting the angle α into Eqn. (16).

Finally, the CoP position can be obtained from:

$$z_{\text{CoP}} = (r_{\text{pad}} - r \cos \alpha) \quad (19)$$

$$y_{\text{CoP}} = r \sin \alpha \quad (20)$$

By substituting the angle α into Eqn. (15), then resolving Eqn. (12) and assuming two rubbing surfaces, the overall brake torque is

$$T_{\text{Brake}} = 2F_t r \quad (21)$$

For a disc brake with the data given in Table 1, the angle α can be calculated as follows

$$\begin{aligned} & \frac{1900.4 + 1900.4}{1 + 0.15 \times 0.4 \cos \alpha} \left(\frac{-0.15 \times 0.4 \cos \alpha (-0.098 + 0.045 \tan \alpha)}{0.15 \times 0.4 + \cos \alpha} \sin \alpha + \dots \right. \\ & \left. + \frac{0.098 - 0.4 \sin \alpha \left(0.0113 + \frac{0.0047}{2} \right)}{0.15 \times 0.4 + \cos \alpha} \sin \alpha + \dots \right) \\ & - 0.4 \cos \alpha \left(0.0113 + \frac{0.0047}{2} \right) - 0.045 \times 0.4 \times 0.15 \cos \alpha + \dots \\ & + 1900.4 \times 0.02 - 1900.4 \times 0.02 = 0 \end{aligned}$$

A numerical solution of the above equation gives

$$\alpha = 0.0834 \text{ rad} = 4.77^\circ$$

Substituting into Eqn. (16) yields the radial distance of CoP

$$r = 97.66 \text{ mm}$$

Table 1: Example of disc brake data for calculation of the CoP position

P_1	1900.4 N (30 bar)
P_2	1900.4 N (30 bar)
d_{piston}	28.4 mm
n_1	20 mm
n_2	20 mm
r_{pad}	98 mm
μ	0.4
μ_A	0.15
t_{fm}	11.3 mm
t_{bp}	4.7 mm
y_A	45 mm

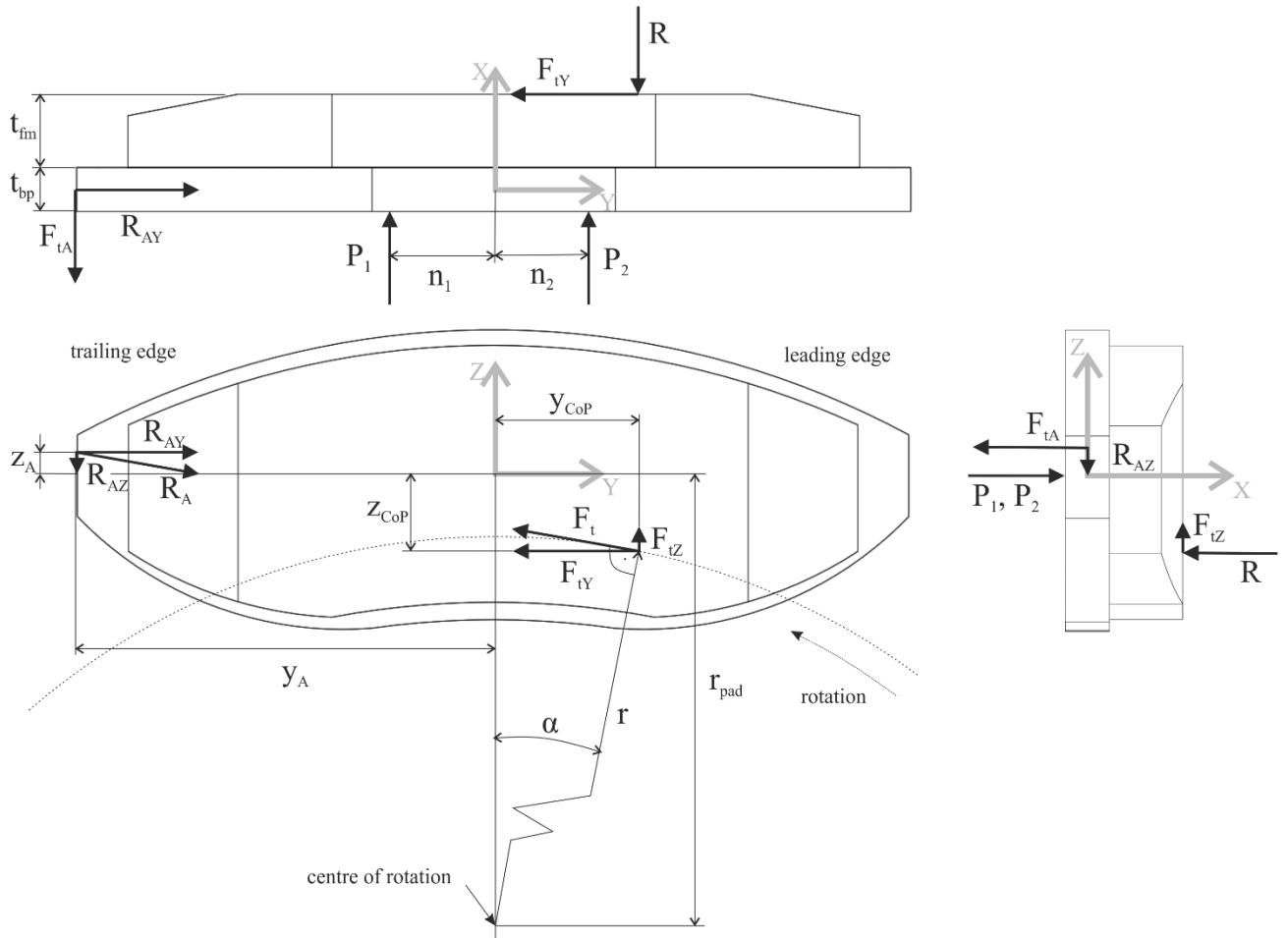


Fig. 2: New 3D analytical model of the brake pad for calculation of the CoP position at the pad/disc interface.

And the brake torque assuming two rubbing areas is

$$T_{\text{Brake}} = 2 \times 1434.6 \times 0.09766 = 280.2 \text{ Nm}$$

2.3. New 3D Analytical Model of the Brake Pad for an 8-Piston Opposed Caliper

Analogously to the four-piston opposed caliper, the equations can be also derived for a caliper with more than four pistons. Without derivation, the resultant equations corresponding to Eqn. (15) - Eqn. (16) for an eight-piston opposed caliper are

$$R = \frac{P_1 + P_2 + P_3 + P_4}{1 + \mu_A \mu \cos \alpha} \quad (22)$$

$$\frac{P_1 + P_2 + P_3 + P_4}{1 + \mu_A \mu \cos \alpha} \left(\frac{-\mu \mu_A \cos \alpha (-r_{\text{pad}} + y_A \tan \alpha) + r_{\text{pad}} - \mu \sin \alpha \left(t_{\text{fm}} + \frac{t_{\text{bp}}}{2} \right)}{\mu \mu_A + \cos \alpha} \right) \sin \alpha + \dots$$

$$+ \frac{P_1 n_{1Z} + P_2 n_{2Z} + P_3 n_{3Z} + P_4 n_{4Z}}{R(\mu \mu_A + \cos \alpha)} \sin \alpha - \mu \cos \alpha \left(t_{\text{fm}} + \frac{t_{\text{bp}}}{2} \right) - y_A \mu \mu_A \cos \alpha - P_1 n_{1Y} - P_2 n_{2Y} - P_3 n_{3Y} - P_4 n_{4Y} = 0 \quad (24)$$

$$r = \frac{-\mu \mu_A \cos \alpha (-r_{\text{pad}} + y_A \tan \alpha)}{\mu \mu_A + \cos \alpha} + \dots + \frac{r_{\text{pad}} - \mu \sin \alpha \left(t_{\text{fm}} + \frac{t_{\text{bp}}}{2} \right)}{\mu \mu_A + \cos \alpha} + \dots + \frac{P_1 n_{1Z} + P_2 n_{2Z} + P_3 n_{3Z} + P_4 n_{4Z}}{R(\mu \mu_A + \cos \alpha)} \quad (23)$$

Finally, analogously to Eqn. (18), the resultant equation can be written as Eqn. (24)

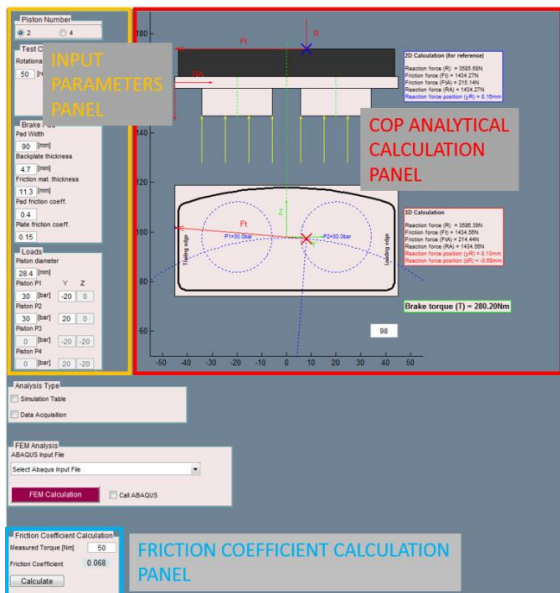


Fig. 3: Analytical calculation of the CoP position using MATLAB[®] program *CalBrakes*.

Again, as from Eqn. (18), the unknown angle α of Eqn. (24) can be calculated numerically. The CoP positions can be determined using Eqn. (19) - Eqn. (20).

The above 2D and 3D analytical models of the brake pad were included in a new MATLAB[®] program *CalBrakes*. Figure 3 shows the main window that is divided into a section where all calculation inputs can be set (Input parameters panel), followed by a section that includes visualization of analytical calculation of the CoP position (CoP analytical calculation panel). The CoP and force values resulting from the 2D calculation serve as a reference to indicate correctness of the 3D model in the circumferential direction. The friction coefficient calculation, which is described in Section 4 below, is performed using the inputs set in the section below the input parameters panel (see Friction coefficient calculation panel in Figure 3).

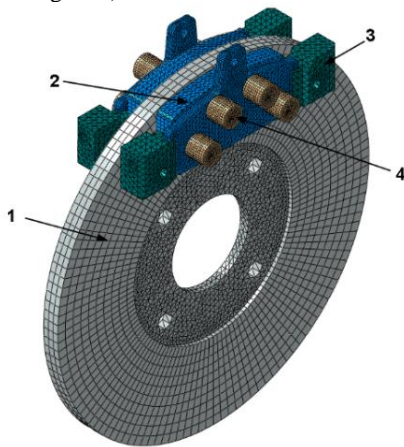


Fig. 4: FE model of an 8-piston opposed disc brake consisting of a: 1) rotor, 2) brake pads, 3) abutments and 4) pistons.

3. Comparison of the New 3D Analytical Model with an Equivalent Finite-Element Model

In this section, the CoP position calculated using the new 3D analytical model is compared with a CoP value resulting from a finite-element (FE) analysis.

In order to induce different CoP positions over the major part of the pad surface, an equivalent model of a disc brake with eight op-

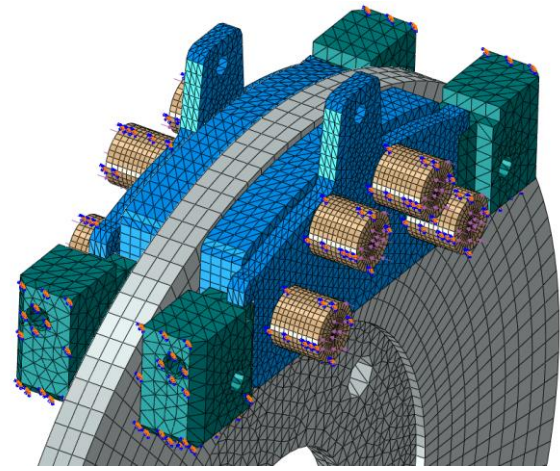


Fig. 5: View of the abutment and piston boundary conditions along with the loads acting on the pistons.

posed pistons allowing independent piston pressure control was developed in ABAQUS[®] as shown in Figure 4.

The FE model consists of a disc rotor, brake pads, abutments and pistons. The caliper is not included in the model, since influence of its geometry is not important for this study. The brake disc is modelled without the top-hat geometry and the flange is mounted symmetrically in the disc section to avoid small differences in CoP positions between the inboard and outboard side of the brake [10]. The disc is given a rotational speed of 50 rev/min and no thermal effects at the pad/disc interface are assumed. Table 2 shows all material properties used in the simulation.

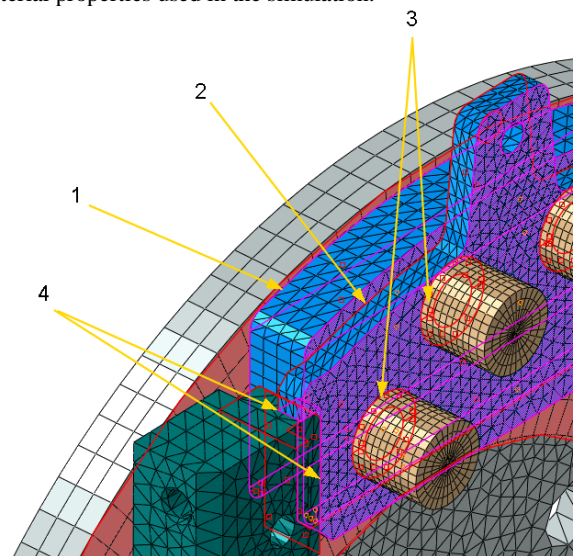


Fig. 6: Detail of the interactions between the components: 1) surface-to-surface contact, small sliding formulation between the disc and the pad friction material, 2) tie constraint between the backplate and the friction material, 3) surface-to-surface contact, finite sliding formulation between the piston and the backplate, 4) surface-to-surface contact, small sliding formulation between the backplate and the abutments.

The brake pad consists of two components, friction material and backplate, both being bonded together with a tie constraint. The thickness of the backplate and the friction material is 4.7 mm and 11.3 mm, respectively. The abutments are modelled as deformable bodies and constrain the pad movement with a surface-to-surface contact and small sliding formulation at the backplate/abutment interface (Figure 5 and Figure 6).

The interaction between the friction material and the brake disc is modelled with the surface-to-surface algorithm and a small sliding formulation is set to save the calculation time.

Table 2: Material specifications used in the FE model.

Part	Material	Density (kg.m ⁻³)	Young's Modulus (GPa)	Poisson's ratio (1)
Brake disc	Cast iron	7200	125	0.24
Pad friction material	Friction material	2700	3	0.25
Backplate	Steel	7850	210	0.3
Abutments	Steel	7850	210	0.3
Pistons	Steel	7850	210	0.3

Also, the piston/backplate interface is modelled as a surface-to-surface contact, but here a finite sliding formulation is used due to otherwise existing convergence problems during the simulation.

The friction coefficient at the brake pad/disc, backplate/pistons and the backplate/abutment interface was set to typical values 0.4, 0.2 and 0.15, respectively. The friction coefficient at the pad/disc interface is ramped from zero to the steady state value at the beginning of the rotation to avoid any discontinuities and convergence problems [11], whereas the friction coefficient at all other surfaces remains constant during the whole simulation.

The piston positions were determined such that they allow placing the CoP almost arbitrarily over the whole pad/disc area while taking into consideration the manufacturability of the piston housing.

Table 3: FE model piston loads.

Load No.	Pressure (bar)			
	p1	p2	p3	p4
1	50	0	0	0
2	5	45	0	0
3	0	0	50	0
4	0	0	5	45
5	12.5	12.5	12.5	12.5
6	20	5	20	5

Table 3 defines piston loads to simulate six different CoP positions across the pad/disc interface. To facilitate the visualization of the CoP results, the MATLAB-ABAQUS interface method as described in [10] was employed. Two different coordinate systems can be used to plot the CoP values as shown in Figure 7. In this paper, the XYZ system located in the disc rotational axis is used as a reference frame. The CoP predictions using the 2D, 3D and FE model for all six load settings are compared in Figure 8. It can be seen that the differences in the CoP positions between all approaches are small for the same load conditions but these positions vary significantly between the different load settings.

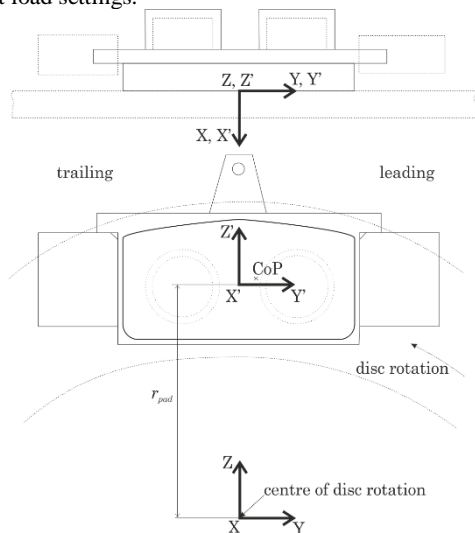


Fig. 7: Axis systems used to display the CoP.

Figure 9 displays the CoP positions determined using the 3D analytical and FE model, as well as pressure distribution contour plots evaluated by the FE model. The CoP position of the 3D model is plotted with the circular marker (o), while the marker (+)

represents calculation of the CoP position using the FE model pressure values at each node according to the following equations:

$$y_{CoP} = \frac{\sum_{i=1}^n p_i(y_i) \times y_i}{\sum_{i=1}^n p_i(y_i)} \tag{26}$$

$$z_{CoP} = \frac{\sum_{i=1}^n p_i(z_i) \times z_i}{\sum_{i=1}^n p_i(z_i)} \tag{27}$$

Due to the identical results for inboard and outboard side of the brake, only one pad/disc interface is illustrated.

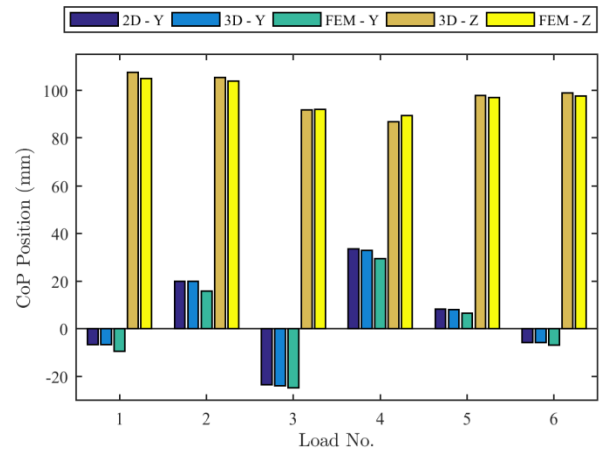


Fig. 8: Comparison of CoP positions calculated using the 2D, new 3D and FE model for six different piston loads.

From Figure 8 and Figure 9 it can be seen that the largest differences of the CoP position tend to be for the load No. 1, 2 and 4 during which the CoP tends to be located towards the leading edge and radially outward from the disc center.

Here, the influence of the missing reaction force at the leading abutment in the analytical pad model seems to be more significant. Table 4 summarises a comparison of the absolute distances of the CoP between the new 3D and FE model, as well as between the 3D and 2D model. Differences greater than 2 mm between the 3D and FE model occur for load cases No. 1, 2 and 4, and the largest difference between the 2D and 3D model is for load case No. 4.

Table 4: Absolute distance of the CoP between 3D and both 2D and FE model.

Load No.	Absolute distance (mm)	
	3D and 2D Model	3D and FEM Model
1	0.0	3.9
2	0.1	4.3
3	0.3	0.9
4	0.7	4.4
5	0.1	1.8
6	0.0	1.7

Table 5 shows results of the pad/disc normal reaction R (clamp force) and friction force F_f calculated by the new 3D, 2D and FE model for all load cases. The friction force F_f differs only slightly across all methods whereas the normal reaction force R determined from the FE model exhibits more significant difference. This can be due to a different behavior of the abutment surface contacts and flexural effects of the pad included in the FE model.

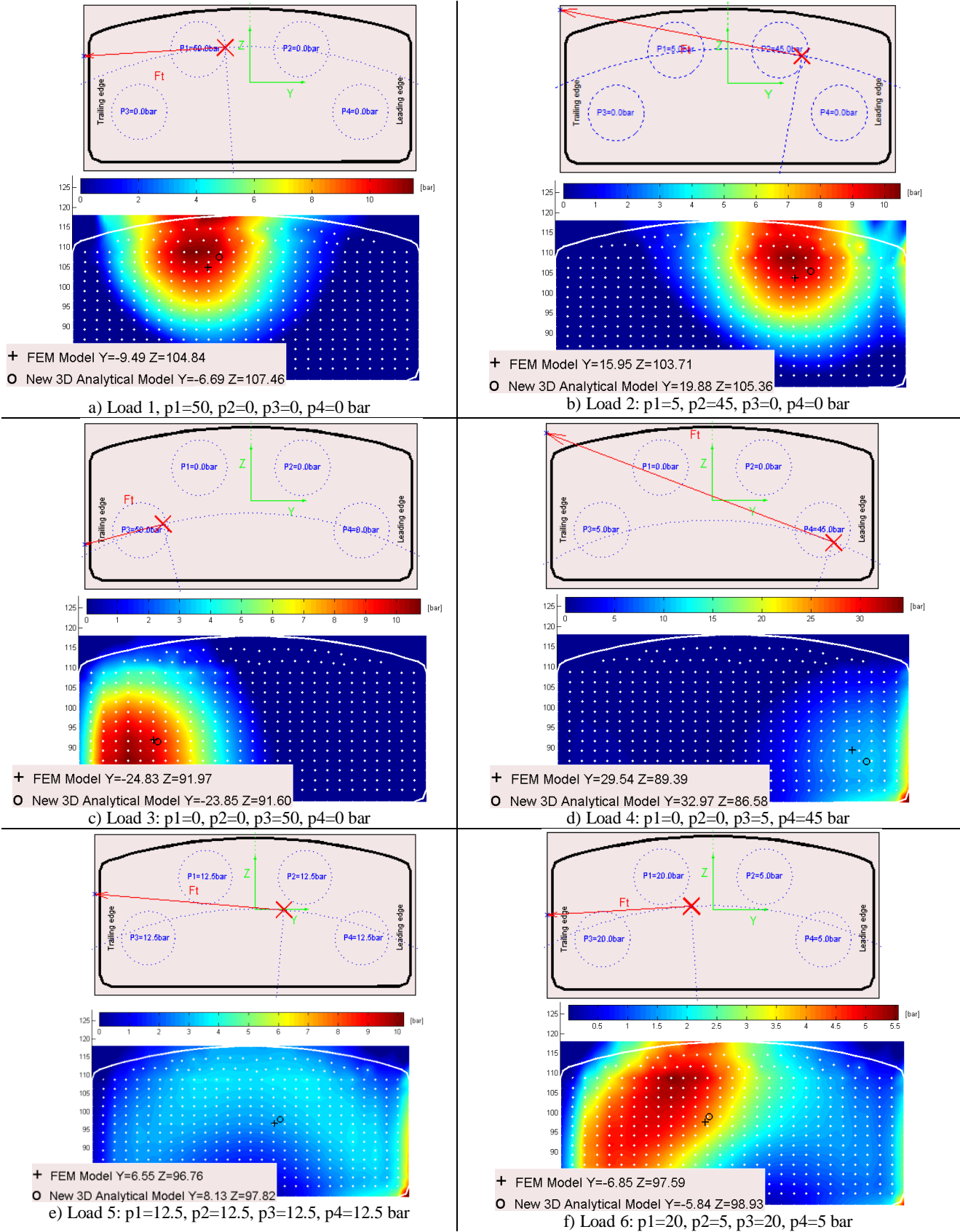


Fig. 9: CoP position and contour plots of the contact pressure for six different piston load settings.

Table 5: Calculated friction F_f and normal reaction R force at the pad/disc interface for six different pressure settings.

Load No.	Piston Pressure [bar]				Force [N]					
					3D Analytical Model		2D Analytical Model		FE Model	
	F_f	R	F_f	R	F_f	R				
1	50	0	0	0	333.5	833.7	333.4	833.6	350.5	885.4

2	5	45	0	0	333.8	834.4	333.4	833.6	346.8	883.4
3	0	0	50	0	334.0	835.1	333.4	833.6	330.8	860.7
4	0	0	5	45	334.7	836.7	333.4	833.6	330.6	875.1
5	12.5	12.5	12.5	12.5	333.5	833.7	333.4	833.6	338.7	874.6
6	20	5	20	5	333.5	833.6	333.4	833.6	339.3	872.4

4. Friction Coefficient Calculation

4.1. Traditional Approach of the Friction Coefficient Calculation

Assuming two rubbing surfaces and the piston actuation force equal to the clamping force, the brake torque at the wheel is calculated using the following formula [12]

$$T_w = 2\mu(p - p_t)A_a \eta r_e \tag{28}$$

where μ is the friction coefficient, p is the actuation pressure, p_t is the threshold pressure, A_a is the total piston area, η is the efficiency of the hydraulic system and r_e is the effective radius. Neglecting the threshold pressure and efficiency of the hydraulic system Eqn. (28) can be written as

$$T_w = 2\mu p A_a r_e \tag{29}$$

The effective radius r_e is assumed to be equal to the mean rubbing radius r_m according to

$$r_e = r_m = \frac{r_o + r_i}{2} \tag{30}$$

where r_o and r_i are the outer and inner radii of the disc rubbing area, respectively.

The effective radius of the brake disc shown in Figure 11 can be calculated using Eqn. (30)

$$r_e = r_m = \frac{118.5 + 77}{2} = 97.75 \text{ mm}$$

To calculate friction coefficient from the given torque and piston pressure data, Eqn. (29) can be rearranged and used in the following form

$$\mu = \frac{T_w}{2pA_a r_e} \tag{31}$$

4.2. Friction Coefficient Calculation Using the New 3D Analytical Model

Here again, the same Eqn. (18) as for the CoP calculation is used to determine the friction coefficient. Since the friction coefficient μ in this equation represents a new unknown parameter, an algorithm containing a simple loop is added, which evaluates possible values of the friction coefficient for a given brake torque. Once the difference between the calculated brake torque and given brake torque is less than an acceptable error value, the loop is terminated and the friction coefficient value is stored. Figure 10 shows a flowchart of the simple loop which was implemented in *CalBrakes* for a rapid friction coefficient evaluation.

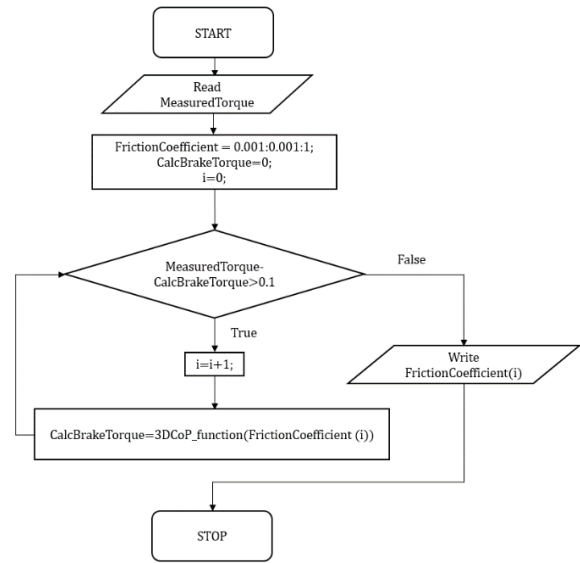


Fig.10: Flowchart of the friction coefficient evaluation using the new 3D analytical model.

4.3. Comparison of the Friction Coefficient Calculation Methods

In this section the new proposed method of the friction coefficient calculation described above is compared with the calculation using the traditional approach. All parameters used in the following calculations are given in Table 6. In the traditional approach the effective radius $r_e = r_m$ and is determined using Eqn. (30), while the new method suggests that the effective radius $r_e = r$ as derived in Eqn. (16). For calculation of the friction coefficient using the new approach, the simple code shown in Figure 10 is implemented in *CalBrakes*, while for the traditional approach Eqn. (31) is used. Table 7 shows a comparison of the mean rotor radius r_m and the radial distance of the CoP r calculated using the 3D model for the friction coefficient $\mu = 0.4$. It is clear, that both methods are independent of the actuation pressure assuming that a uniform piston load is used.

Table 6: Data used for the friction coefficient calculation.

Traditional approach Eqn. (31)		3D model	
A_a	1266.94e-6 m ²	A_n	1266.94e-6 m ²
r_e	97.75 mm	n_1	20 mm
		n_2	20 mm
		r_{pad}	98 mm
		μ_A	0.15
		t_{fm}	11.3 mm
		t_{bp}	4.7 mm
		y_A	45 mm

The brake assembly setup shown in Figure 11 was used to conduct drag brake tests for a range of brake line pressures. The brake assembly consists of a four-piston opposed laboratory caliper, a solid rotor, a pair of brake pads, mounting brackets and an inlet brake piping. A constant rotational speed of 155 rpm is set for all testing procedures.

Table 7: Comparison of the effective radii calculated the traditional way and using the 3D model for four brake line pressure values.

Brake line pressure (bar)	r_m (mm) Eqn. (30)	r (mm) 3D model ($\mu = 0.4$)
2.5	97.75	97.66
5		
7.5		
10.0		

During the braking event, a torque sensor mounted in the dynamometer shaft collects the torque data and a pressure transducer monitors the brake line pressure. The disc temperature is recorded using a sliding thermocouple. For all brake line pressure values, special care is taken to collect all data within a certain temperature range, in this case a range of 100-120°C was chosen, to avoid differences in brake torque values that might otherwise arise due to the friction coefficient dependency on temperature.



Fig. 11: The brake assembly setup used for drag brake testing procedures.

Figure 12 shows a comparison of the friction coefficient values calculated using both methods for four different brake line pressures: 2.5, 5, 7.5 and 10 bar. The measured torque and actuation pressure were collected from the measurements on the brake dynamometer as shown in Figure 11.

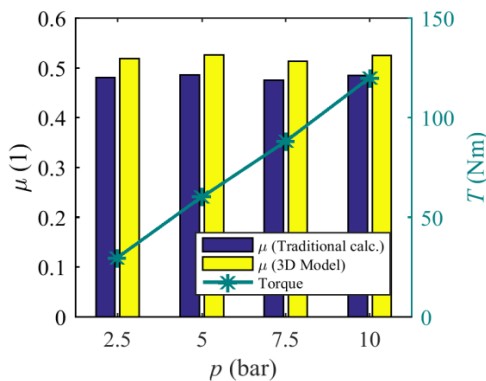


Fig. 12: Comparison of the friction coefficient values calculated using the traditional method and the new 3D model.

The new 3D model gives an approximately 8% greater value of the friction coefficient than the value determined using the traditional method. The difference is due to the greater complexity and accuracy of the new 3D model which is included in the proposed calculation method. Although both methods give similar values of the effective radius r_e , the higher value of the friction coefficient stems predominantly from differences in the reaction force R calculation that for the 3D approach depends on a more complex relation according to Eqn. (15).

5. Conclusion

The paper presents a new three-dimensional (3D) rigid body model of the brake pad which is used to calculate centre of pressure (CoP) position in both circumferential and radial directions during a constant speed braking event. This mathematical model can be used to determine the CoP position and other parameters in a trailing abutment brake pad loaded with different numbers of pistons. A number of CoP positions for different pressure load settings were compared with the CoP positions evaluated from a detailed finite-element model of an equivalent disc brake. The results showed a close correlation between these two approaches, giving the new analytical model a potential use in applications where an instantaneous value of the CoP with good accuracy is required. Finally, the new analytical model was used to calculate the friction coefficient using data acquired from drag brake tests on a brake dynamometer. A comparison of the results collected from the brake dynamometer tests showed that the new 3D model gives an approximately 8% larger value of the friction coefficient than the friction coefficient calculated the traditional way. The advantage of the new proposed approach is that it yields more accurate values of the effective radius compared to the mean radius used in the traditional approach. Also, the reaction (clamp) force calculation includes a greater degree of complexity. Since the real value of the friction coefficient is not known, this new method cannot be proved in terms of absolute accuracy. However, it does represent a different approach to how a friction coefficient can be calculated. Ongoing research aims to identify other practical applications where the new 3D analytical model of the brake pad can be used and further developed, such as in the prediction of brake squeal.

References

- [1] Papinniemi A., Lai J. C., Zhao J., and Loader L. 2002. Brake squeal: a literature review. *Applied acoustics*. 63(4): 391-400.
- [2] Savant Rushikesh D., S. Y. Gajjal, and V. G. Patil. 2014. Review on Disc Brake Squeal. *International Journal of Engineering Trends and Technology*. 9(12): 605-608.
- [3] Fieldhouse J. D., Ashraf N., and Talbot C. J., 2009. The measurement and analysis of the disc/pad interface dynamic centre of pressure and its influence on brake noise. *SAE International Journal of Passenger Cars - Mechanical Systems*. 1(1): 736-745.
- [4] Kim J. Y., Kim J., Kim Y. M., Jeong W., and Cho H. 2015. An Improvement of Brake Squeal CAE Model Considering Dynamic Contact Pressure Distribution. *SAE International Journal of Passenger Cars - Mechanical Systems*. 8(4): 1188-1195.
- [5] Park J. S., Han M. G., and Oh S. Y. 2016. A Study of the Relationship between Leading Offset and Squeal Noise. *SAE International Journal of Passenger Cars - Mechanical Systems*. 9(3): 1144-1150.
- [6] Newcomb T. P., and Spurr R. T. 1967. *Braking of road vehicles*. Chapman & Hall. ISBN 0412092700.
- [7] Fieldhouse J. D., Ashraf N., and Talbot, C. J., Pasquet T., Franck P. and Gabriel R. 2006. Measurement of the dynamic center of pressure of a brake pad during a braking operation. *SAE Technical Paper 2006-01-3208*.
- [8] Neis D. P., Duarte F. L., Perez D.Y., Ferreira N. F., and DeBaets, P. 2012. Methodology for determination of the effective radius by means of thermograph analysis on the disk surface. In: *EuroBrake Conference Proceedings*.
- [9] Lange J., Degenstein T., Dohle A., and Elvenkemper A. 2006. Der μ -Wert Reibwert-bestimmung in Bremssystemen. In: *XXVI*.

- Internationales μ -Symposium 2006, Fortschritt-Berichte VDI Reihe 12 Nr. 620, ISBN 3-1836-2012-X.
- [10] Budinsky T., Brooks P., Barton D. 2017. The influence of disc geometry on the centre of pressure and squeal propensity for an automotive disc brake. In: EuroBrake Conference Proceedings.
- [11] Abaqus 6.12, 2012. Example Problems Manual, Volume I: Static and Dynamic Analyses, https://things.maths.cam.ac.uk/computing/software/abaqus_docs/docs/v6.12/pdf_books/EXAMPLES_1.pdf
- [12] Day A. 2014. Braking of road vehicles. Butterworth-Heinemann. ISBN 978012397314-6.